Acta Cryst. (1996). A52, 717-729

Electron Statistical Dynamical Diffuse Scattering in Crystals Containing Short-Range-Order Point Defects

Z. L. WANG

School of Material Science and Engineering, Georgia Institute of Technology, Atlanta, GA 30332-0245, USA. E-mail: zhong.wang@mse.gatech.edu

(Received 1 February 1996; accepted 25 April 1996)

Abstract

A formal statistical dynamical theory is developed to calculate diffuse scattering produced by short-range order (SRO) in a distorted crystal structure with consideration of atomic thermal vibrations. Diffuse scattering not only produces fine details in diffraction patterns but also introduces a non-local imaginary potential function that reduces the intensities of the Bragg reflected beams. The distribution of the diffusely scattered electrons and the Fourier coefficients of the absorption potential are directly related to a dynamic form factor $S(\mathbf{Q},\mathbf{Q}')$, which has been calculated with consideration of SRO in the distorted lattices. The statistical structure average on imperfections is performed analytically and the final result is correlated to Cowley's short-range-order parameters. The theory is formulated in the Bloch-wave scheme (Bethe theory) for the convenience of numerical calculation in transmission electron diffraction. A rigorous theoretical proof is given to show that the inclusion of a complex potential in the dynamical calculation automatically recovers the contributions made by the high-order diffuse scattering, although the calculation is done using the equation derived for single diffuse scattering. This simply expands the capability of conventional single diffuse scattering theories. Therefore, the complex potential has a much richer meaning than the conventional interpretation of absorption effect.

1. Introduction

The study of point defects is becoming increasingly important in the characterization of advanced functional materials. We take $La_{1-x}Ca_xMnO_3$ (LCMO), a material that has been found to exhibit a colossal magnetoresistance (CMR) effect (Jin, Tiefel, McCormack, Fastnacht, Ramech & Chen, 1994), as an example. An ordered lattice substitution of La^{3+} by Ca^{2+} creates excess local negative charge, which is balanced partly by the valence conversion of Mn^{3+} into Mn^{4+} and partly by creation of oxygen vacancies (Jonker & van Santen, 1953), thus the charge structure of LCMO is

$$La^{3+}_{1-x}Ca^{2+}_{x}Mn^{3+}_{1-x+2y}Mn^{4+}_{x-2y}O^{2-}_{3-y}V^{O}_{y},$$

where V^{O}_{y} stands for the ratio of oxygen vacancies. The conductivity of LCMO is due to the transfer of electrons between Mn^{3+} and Mn^{4+} (Zener, 1951), and the transfer probability of the electrons is directly related to the angle Θ_{ij} between the spins of the Mn ions (Anderson & Hasegawa, 1955; De Gennes, 1960), possibly resulting in the dependence of the electric conductivity of LCMO on the strength of the applied magnetic field (*i.e.* the magnetoresistance effect).

Determination of the short-range-order (SRO) structure of oxygen vacancies, however, is a challenge to existing structure-analysis techniques. Transmission electron microscopy, as a technique for probing the crystallographic structure of small crystals (for reviews, see Spence & Zuo, 1992; Cowley, 1992, 1993), is likely to play a unique role in determining crystal structures containing modulated (or distorted) lattices (Amelinkx & Van Dyck, 1993; Gjønnes, 1993). Recent studies of SRO of oxygen vacancies in cubic ZrO_2 stabilized by Y_2O_3 and MgO by electron diffraction have demonstrated its experimental feasibility (Dai, Wang, Chen, Wu & Liu, 1996; Dai, Wang & Liu, 1996). In addition, progress in instrumentation has made it possible to filter off contributions made by electrons that have suffered energy losses larger than a few eV (for a review, see the book edited by Reimer, 1995), thus, quantitative structure determination using the energy-filtered electron diffraction and image information is a future direction of electron microscopy. Quantitative microscopy is possible only when a well established theory is available. Even though there are several approaches that have been developed to solve the Schrödinger equation for high-energy electron diffraction (for reviews, see Cowley, 1995; Wang, 1995*a*), the Bethe theory (Bethe, 1928) and the multislice theory (Cowley & Moodie, 1957) are the most useful ones. The Bloch-wave theory is best suited for calculating diffraction patterns of a periodically structured crystal; the multislice theory is an optimum choice for simulations of high-resolution transmission-

electron-microscopy (HRTEM) images of crystals containing defects. HRTEM images recorded from a crystal containing SRO structure can be properly calculated using the multislice theory (De Meulenaere, Van Dyck, Van Tendeloo & Van Landuyt, 1995; Van Dyck, 1985) because the atom arrangement in each slice can be chosen differently. Diffraction data recorded from a crystal containing SRO of point defects, however, cannot be calculated using the Bloch-wave theory because of the non-periodic crystal structure. Moreover, the perturbation produced by SRO on crystal structure can vary from unit cell to unit cell, thus a statistical dynamical diffraction theory is required.

The statistical dynamical diffraction theory has been proposed (Kato, 1980, 1991; Becker & Al Haddad, 1990, 1992) based on the Takagi–Taupin equations (Takagi, 1962; Taupin, 1964). The theory was developed to deal specifically with the propagation of the average Bragg beam amplitudes at the presence of statistical imperfections in the crystal, but the diffuse scattering produced by the imperfections was not calculated. Although the kinematical diffuse scattering theory of crystals containing point defects has been developed for many years (Borie, 1957, 1959; Hayakawa & Cohen, 1975; Cowley, 1995), the dynamical theory needed for quantitative data analysis is still at an early stage. The multislice theory of Cowley & Moodie (1957) has been applied to perform dynamical calculations of electron diffraction of TDS and SRO (Cowley & Pogany, 1968), in which a large unit cell and a variety of different crystal slices need to be constructed in order to account for the spatial variation in the distribution of point defects, provided pre-knowledge of the real-space distribution of the SRO point defects is available.

In this paper, a new theoretical scheme is proposed to calculate diffuse scattering patterns generated by SRO and atomic thermal vibrations in crystal lattices. After reviewing the diffuse scattering in electron diffraction (§2), a general theory is proposed to calculate the statistical diffraction intensity of diffusely scattered electrons (§3). This theory is given in the Bloch-wave representation best suited for numerical calculations. It is proved that the calculation of diffuse scattering is entirely determined by a dynamic form factor $S(\mathbf{Q},\mathbf{Q}')$. The calculations of this factor for two cases involving SRO of point defects are given in §4. Finally, the absorption potential introduced by thermal diffuse scattering (TDS) and SRO is also derived and its role in recovering the high-order diffuse scattering is proved rigorously (§5).

2. Diffuse scattering in electron diffraction

Diffuse scattering is produced by structure modulation in a crystalline specimen, and it is usually distributed between Bragg reflected peaks. The Bragg reflections are generated by the periodically structured lattice of the crystal, while the diffuse scattering is produced by the non-periodical components including thermal vibrations of the crystal atoms and SRO of defects. Thermal diffuse scattering (TDS) exists even for a perfect crystal without defects because atomic vibration is a non-periodic perturbation on the crystal potential. Fig. 1 shows an electron diffraction pattern recorded at 200 kV from an Ag foil. The TDS streaks observed in the pattern are determined by phonon dispersion relations of the acoustic branches (Honjo, Kodera & Kitamura, 1964; Komatsu & Teramoto, 1966; Wang, 1992). A general feature in the TDS diffraction pattern is that all the streaks run along the lines interconnecting the Bragg peaks. For a monoatomic cubic structure, a simple rule has been proposed to directly predict the directions of the streaks in diffraction patterns from the unit-cell structure of the crystal (Wang & Bentley, 1991). This is a distinct difference from the diffuse scattering produced by SRO of point defects, as shown in Fig. 2. Dynamical theories for calculations of diffraction patterns and images of TDS electrons have been extensively developed based on the multislice approach (Cowley, 1988; Fanidis, Van Dyck, Coene & Van Landuyt, 1989; Coene & Van Dyck, 1990; Fanidis, Van Dyck & Van Landuyt, 1992; Wang, 1990, 1992, 1995*b*; Wang & Bentley, 1991; Dinges, Berger & Rose, 1995), the Bloch-wave approach (Rossouw, 1985; Rossouw & Bursill, 1985) and the Green-function approach (Dudarev, Peng & Ryazanov, 1991; Wang & Li, 1995).

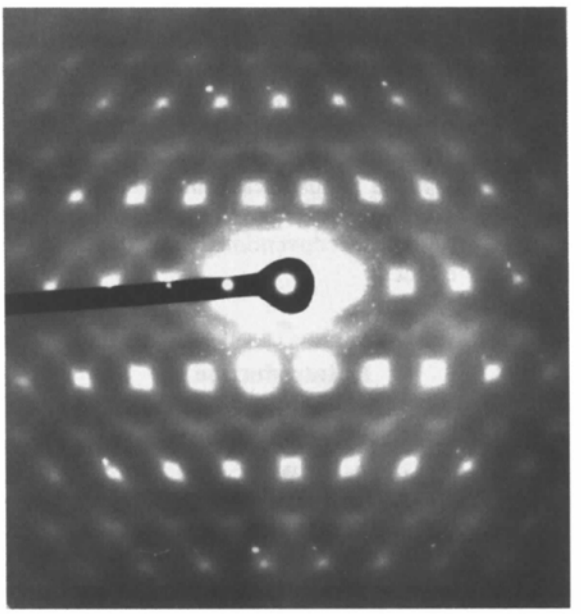

Fig. 1. A (013) electron diffraction pattern recorded from a thin Ag foil showing many diffuse scattering streaks caused by thermal diffuse scattering.

Fig. 2 shows a diffuse scattering pattern recorded from a cubic ZrO_2 stabilized by Y_2O_3 and MgO. The diffuse scattering pattern is produced by the oxygen-vacancy short-range order (Dai, Wang, Chen, Wu & Liu, 1996). The distribution of diffuse scattering intensity is rather complex and a three-dimensional geometrical model in reciprocal space is established for describing the equal-intensity contours of diffuse scattering observed experimentally. The intensity pattern reflects the correlation and order of oxygen vacancies in the specimen. Electron diffraction is probably the most sensitive and localized technique that can be applied to study SRO of point vacancies, which is an important aspect in studying oxide functional materials because the variation of cation valences is compensated by creating oxygen vacancies. A detailed study of this pattern has been performed using the kinematical scattering theory (Dai, Wang & Liu, 1996).

In general, the diffuse scattering created by SRO cannot be easily separated experimentally from that produced by TDS. It is thus necessary to include both processes in theoretical calculations. The theory proposed in this paper is designated for this purpose.

3. A general approach

To include in calculation the effects produced by atomic thermal vibrations and structure distortion due to SRO, ones uses a general approach in which an *average crystal structure* is introduced (Takagi, 1958; Cowley, 1995). The crystal potential $V(\mathbf{r}, t)$ is written in the form

$$V(\mathbf{r}, t) = V_0(\mathbf{r}) + \Delta V(\mathbf{r}, t), \tag{1}$$

where $V_0(\mathbf{r}) = \langle V(\mathbf{r}, t)\rangle_{ts}$ is the crystal potential for the average lattice, defined to be time independent and periodic, $\langle\ \rangle_{ts}$ indicates the statistical time and structure average and $\Delta V(\mathbf{r})$ represents the deviation from the average lattice with $\langle \Delta V(\mathbf{r}, t)\rangle_{ts} = 0$, which is non-periodic and time dependent (for TDS). The statistical structure average $\langle\ \rangle_s$ is introduced to take into account the SRO in the crystal structure. The statistical time average is to consider the variation in thermal vibration configurations of crystal lattices. The physical picture contained in (1) is schematically shown in Fig. 3 using a one-dimensional potential model, where only SRO is considered. For a crystal containing point vacancies, the crystal potential can be separated into a periodic component (V_0) and a deviation term ΔV (Fig. 3*a*). Similar mathematical treatment can be adopted for a binary crystal in which atom substitutions between the *A* and *B* types of atom can occur (Fig. 3*b*). The separation of V_0 from ΔV has a powerful application in describing crystals containing point defects using the Patterson function (Cowley, 1995).

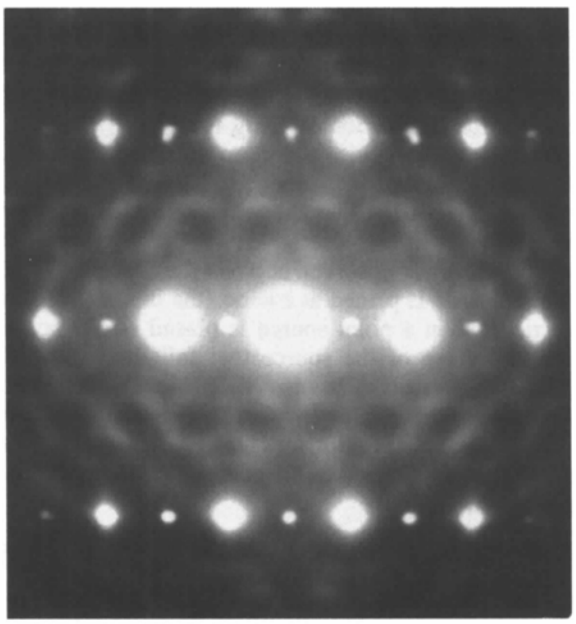

Fig. 2. A (013) electron diffraction pattern recorded at 120 kV from cubic ZrO_2 stabilized by Y_2O_3 and MgO showing diffuse scattering created by oxygen vacancies in the crystal (courtesy of Dr Z. R. Dai).

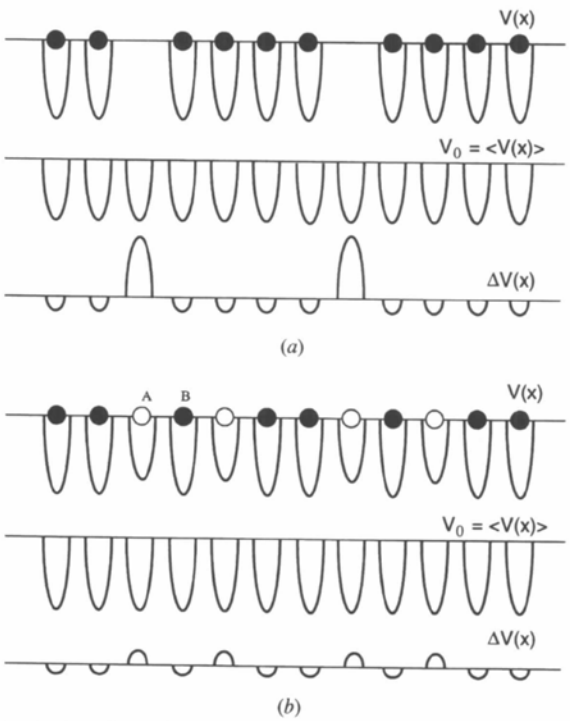

Fig. 3. One-dimensional representation of crystal potential V, the structurally averaged potential $V_0 = \langle V\rangle$ and the deviation potential $\Delta V = V - V_0$ for (*a*) a crystal containing point vacancies and (*b*) a binary alloy with atom substitutions between the *A* and *B* types of atom. V_0 is a periodic function but ΔV is not.

In high-energy electron scattering, the 'frozen' lattice model is assumed in describing TDS. Since the interaction time between an incident electron with a thin specimen is much shorter than the vibration period of an atom, the crystal atoms are seen as stationary by the incident electron. An electron diffraction pattern or image is considered to be a statistical average over the scattering intensities for many instantaneous pictures of the displaced atoms (Hall & Hirsh, 1965). The first objective in our theory is to find the scattered electron wave function for a given frozen lattice configuration, then a statistical time average is made on the electron diffraction intensities for a vast number of different thermal vibration configurations. For simplicity, we start from the time-independent Schrödinger equation with relativistic correction (Humphreys, 1979; Spence, 1988),

$$[-(\hbar^2/2m_0)\nabla^2 - e\gamma V_0 - e\gamma\Delta V - E]\Psi = 0, \quad (2)$$

where $E = eU_0[1 + eU_0/2m_0c^2]$, U_0 is the accelerating voltage of the electron microscope, the relativistic factor $\gamma = (1 - v^2/c^2)^{-1/2}$ and v is the electron velocity. For diffraction calculation, the Green-function theory is the most convenient choice (Kainuma, Kashiwase & Kogiso, 1976; Wang & Li, 1995). If the ΔV term is shifted to the right-hand side, (2) is converted into an integral equation with the use of Green's function $G(\mathbf{r}, \mathbf{r}_1)$:

$$\Psi(\mathbf{r}, t) = \Psi_0(\mathbf{K}_0, \mathbf{r}) + \int d\mathbf{r}_1 G(\mathbf{r}, \mathbf{r}_1)[e\gamma\Delta V(\mathbf{r}_1, t)\Psi(\mathbf{r}_1, t)], \quad (3)$$

where G is the solution of

$$[-(\hbar^2/2m_0)\nabla^2 - e\gamma V_0 - E]G(\mathbf{r}, \mathbf{r}_1) = \delta(\mathbf{r} - \mathbf{r}_1) \quad (4)$$

and $\Psi_0(\mathbf{K}_0, \mathbf{r})$ is the elastic wave scattered by the periodic time-independent average potential V_0 due to an incident plane wave with wave vector $\mathbf{K}_0$ and satisfies

$$[-(\hbar^2/2m_0)\nabla^2 - e\gamma V_0 - E]\Psi_0 = 0. \quad (5)$$

Equation (5) can be solved using the Bloch-wave or multislice theory. It must be pointed out that the time variable in (3) represents the instantaneous lattice configuration of the crystal due to thermal vibration.

When the observation point is at infinity, the observed diffraction pattern is the squared modulus of the Fourier transform (FT) of $\Psi(\mathbf{r})$. In (3), the diffraction amplitude due to the periodic potential V_0 is calculated from the first term:

$$\begin{aligned}\Phi_0(\mathbf{u}_b) &= \int dx \int dy \exp[-2\pi i(u_x x + u_y y)]\, \Psi_0(\mathbf{K}_0, x, y, \infty) \\ &= \mathrm{FT}[\Psi_0(\mathbf{K}_0, x, y, \infty)], \end{aligned} \quad (6)$$

where $\mathbf{u}_b = (u_x, u_y)$ is a two-dimensional reciprocal-space vector perpendicular or nearly perpendicular to the incident-beam direction (see Fig. 4*a*). $\Phi_0(\mathbf{u}_b)$ is responsible for the intensity of the Bragg reflections. The diffraction due to the non-periodic potential ΔV is represented by

$$\Delta\Phi(\mathbf{u}_b) = \int d\mathbf{r}_1 \hat{G}(\mathbf{u}_b, \infty, \mathbf{r}_1)[e\gamma\Delta V(\mathbf{r}_1, t)\Psi(\mathbf{r}_1, t)], \quad (7)$$

where $\hat{G}(\mathbf{u}_b, \mathbf{r}_1) = \mathrm{FT}[G(x, y, z = \infty, \mathbf{r}_1)]$. $\Delta\Phi(\mathbf{u}_b)$ is responsible for the diffuse scattering observed in the electron diffraction pattern. The diffraction pattern is calculated under the first-order diffuse scattering approximation: $\Psi(\mathbf{r}_1, t)$ is replaced by $\Psi_0(\mathbf{K}_0, \mathbf{r}_1)$ in (7) to give

$$\begin{aligned}\Psi(\mathbf{r}, t) \simeq \Psi_0(\mathbf{K}_0, \mathbf{r}) &+ \int d\mathbf{r}_1 G(\mathbf{r}, \mathbf{r}_1) \\ &\times [e\gamma\Delta V(\mathbf{r}_1, t)\Psi_0(\mathbf{K}_0, \mathbf{r}_1)]. \end{aligned} \quad (8a)$$

This approximation holds if the diffuse scattering is much weaker than the Bragg reflections. However, as will be shown in §5, the high-order diffuse scattering terms dropped by this approximation can be recovered by a correction potential to enable (8*a*) to be applied to cases where the disorder is high. This result also applies to the discussions illustrated below. The diffuse scattering intensity is calculated by

$$\begin{aligned} I_D(\mathbf{u}_b) &= \langle |\Delta\Phi(\mathbf{u}_b)|^2 \rangle_{ts} \\ &= e^2\gamma^2 \int d\mathbf{r}_1 \int d\mathbf{r}_2 \hat{G}(\mathbf{u}_b, \mathbf{r}_1)\hat{G}^*(\mathbf{u}_b, \mathbf{r}_2) \\ &\quad \times \langle \Delta V(\mathbf{r}_1, t)\Delta V^*(\mathbf{r}_2, t) \rangle_{ts} \\ &\quad \times \Psi_0(\mathbf{K}_0, \mathbf{r}_1)\Psi_0^*(\mathbf{K}_0, \mathbf{r}_2), \end{aligned} \quad (8b)$$

where the contributions made by different instantaneous crystal lattices due to thermal vibrations is represented by a time average $\langle\ \rangle_t$; the structure average $\langle\ \rangle_s$ is to statistically average on imperfections introduced by SRO. The most important advantage of this equation is that the time and structure average can be performed analytically before numerical calculations. We now consider the calculation of $\hat{G}(\mathbf{u}_b, \mathbf{r}_1)$.

From the reciprocity theorem, $G(x, y, z = \infty, \mathbf{r}_1) = G(\mathbf{r}_1, x, y, z = \infty)$, provided there is no absorption. This relation means that the wave observed at $z = \infty$ when a point source is placed at $\mathbf{r}_1$ in the specimen is the same as the wave observed at $\mathbf{r}_1$ (in the specimen) when a point source is placed at $z = \infty$ (the image plane). In practice, when a point source is placed at $z = \infty$, the spherical wave of the source that falls on the crystal surface is equivalent to a plane wave, thus, $G(\mathbf{r}_1, x, y, z = \infty)$ is equivalent to the solution of the Schrödinger equation for an incident plane wave. This relation can be proved mathematically (Dudarev, Peng & Whelan, 1993) as

$$\hat{G}(\mathbf{u}_b, \mathbf{r}_1) = A_z\Psi_0(-\mathbf{K}_0 - \mathbf{u}_b, \mathbf{r}_1), \quad (9)$$

where $\Psi_0(-\mathbf{K}, \mathbf{r}_1)$ is the solution of the Schrödinger equation [equation (5), which will be replaced by (48) with the inclusion of the absorption effect] for an incident plane wave vector $(-\mathbf{K})$ $(\mathbf{K} = \mathbf{K}_0 + \mathbf{u}_b)$ and $A_z = -[im_0 \exp(2\pi i K_z z)](\pi\hbar^2 K_z)^{-1}$. The negative sign of

the wave vector means that the electron strikes the crystal along the negative z-axis direction, as schematically shown in Fig. 4(*b*). Equation (9) is a key relation, which makes the calculation of the Green function so convenient. The elastic scattering wave $\Psi_0(-\mathbf{K}, \mathbf{r}_1)$ can be obtained using conventional dynamical approaches, such as the Bethe theory. Thus,

$$I_D(\mathbf{u}_b) = D\int d\mathbf{r}_1 \int d\mathbf{r}_2 \Psi_0(-\mathbf{K}_0-\mathbf{u}_b, \mathbf{r}_1)\Psi_0^*(-\mathbf{K}_0-\mathbf{u}_b, \mathbf{r}_2) \times \langle \Delta V(\mathbf{r}_1, t)\Delta V^*(\mathbf{r}_2, t)\rangle_{ts} \times \Psi_0(\mathbf{K}_0, \mathbf{r}_1)\Psi_0^*(\mathbf{K}_0, \mathbf{r}_2) \quad (10)$$

with $D = e^2\gamma^2 m_0[2\pi^2 h^2 E\cos^2\varphi_0]^{-1}$, where φ_0 is the angle between $\mathbf{K}$ and the z axis. In general, $\langle \Delta V(\mathbf{r}_1, t)\Delta V^*(\mathbf{r}_2, t)\rangle_{ts}$ is written into a Fourier transform form:

$$\langle \Delta V(\mathbf{r}_1, t)\Delta V^*(\mathbf{r}_2, t)\rangle_t = \int d\mathbf{Q} \int d\mathbf{Q}' \exp[2\pi i(\mathbf{r}_1\cdot\mathbf{Q} - \mathbf{r}_2\cdot\mathbf{Q}')]\, S(\mathbf{Q}, \mathbf{Q}'), \quad (11)$$

where $S(\mathbf{Q}, \mathbf{Q}')$ is defined as the diffuse scattering dynamic form factor. Thus, (10) is rewritten as

$$I_D(\mathbf{u}_b) = D\int d\mathbf{Q} \int d\mathbf{Q}' S(\mathbf{Q}, \mathbf{Q}') \times \{\mathrm{FT}[\Psi_0^*(-\mathbf{K}_0 - \mathbf{u}_b, \mathbf{r}_1)\Psi_0^*(\mathbf{K}_0, \mathbf{r}_1)]|_{\mathbf{Q}}\}^* \times \{\mathrm{FT}[\Psi_0^*(-\mathbf{K}_0 - \mathbf{u}_b, \mathbf{r}_2)\Psi_0^*(\mathbf{K}_0, \mathbf{r}_2)]|_{\mathbf{Q}'}\}, \quad (12)$$

where the subscripts $\mathbf{Q}$ and $\mathbf{Q}'$ mean that the variables of the transformed functions are $\mathbf{Q}$ and $\mathbf{Q}'$, respectively. Since Ψ_0 can be calculated using the existing elastic scattering theories for the average periodic crystal potential V_0, the key step in the diffuse scattering calculation is to find the $S(\mathbf{Q}, \mathbf{Q}')$ function. The role played by $S(\mathbf{Q}, \mathbf{Q}')$ in diffuse scattering is analogous to that played by the crystal potential in elastic scattering.

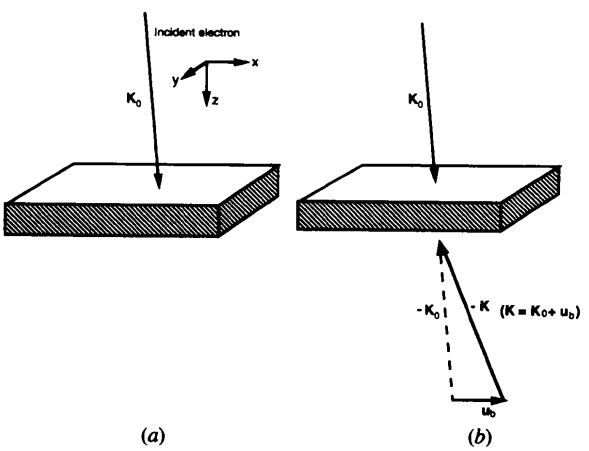

Fig. 4. (*a*) A coordinate system used to describe transmission electron diffraction by a thin slab crystal. The incident beam is nearly parallel to the z axis, the $\mathbf{b} = xy$ plane is the surface of the crystal slab. $\mathbf{K}_0$ is parallel or nearly parallel to the z axis. (*b*) A schematic diagram showing the calculation of $\Psi_0(-\mathbf{K}, \mathbf{r}_1)$ according to the reciprocity theorem.

Equation (12) is a general equation, which has been applied to calculate the diffuse scattering produced by atomic vibrations and point vacancies in a growing surface in reflection high-energy electron diffraction (Wang, 1996*a*). In this paper, this equation is applied to calculate the diffraction of transmitted electrons. We now consider the diffraction of an incident plane wave. An electron wave function in a periodically structured lattice described by the average potential V_0 can be obtained using the Bethe theory. In the Bloch-wave representation, the elastic scattering wave of incident wave vector $\mathbf{K}$ is a linear superposition of Bloch waves $B_i(\mathbf{K}, \mathbf{r})$,

$$\Psi_0(\mathbf{K}, \mathbf{r}) = \sum_i \alpha_i(\mathbf{K})B_i(\mathbf{K}, \mathbf{r}), \quad (13a)$$

where

$$B_i(\mathbf{K}, \mathbf{r}) = \sum_g C_g^{(i)}(\mathbf{K})\exp[2\pi i(\mathbf{K}+\mathbf{g})\cdot\mathbf{r} + 2\pi i\nu_i z], \quad (13b)$$

α_i are the superposition coefficients determined by the boundary conditions, and $C_g^{(i)}$ and ν_i are the Bloch-wave coefficients and eigenvalue of the ith Bloch wave $B_i(\mathbf{K}, \mathbf{r})$, respectively. For a periodically structured crystal, the crystal potential can be written in a Fourier series, thus, (5) is converted into a set of coupled algebra equations (Humphreys, 1979; Spence & Zuo, 1992) by

$$[2KS_g - 2(K_z + g_z)\nu]C_{\mathbf{g}} + (2\gamma m_0 e/h^2)\sum_{\mathbf{h}} V_{\mathbf{g}-\mathbf{h}}C_{\mathbf{h}} \simeq 0, \quad (14)$$

where $V_{\mathbf{g}}$ are the Fourier coefficients of the average crystal potential V_0 and $S_{\mathbf{g}}$ is the excitation error of the $\mathbf{g}$ reflection. Equation (14) can be solved using the matrix diagonalization technique. For a thin parallel-sided crystal slab, the α_i coefficients are determined by the boundary conditions $\alpha_i = C_0^{(i)*}$ if the absorption potential is zero and $\alpha_i = C_{I0}^{(i)}$ if the absorption effect is included, where $C_{I0}^{(i)}$ are the elements of the first column of the inverse of the matrix whose elements are $C_{\mathbf{g}}^{(i)}$ (row i and column $\mathbf{g}$). The Bloch-wave theory has shown remarkable success in describing transmission electron diffraction. The theory can be applied to precisely calculate the rocking curves obtained in convergent-beam electron diffraction, making it possible to determine the bonding-charge distribution in crystalline specimens (Zuo, Spence & O'Keefe, 1988). The Fortran program developed by Spence & Zuo (1992) solves (14) numerically for any crystallographic system.

For diffuse scattering, substituting (13) into (12) and performing the integrals gives the TDS intensity at $\mathbf{u}_b$ in reciprocal space:

$$I_D(\mathbf{u}_b) = D\sum_i\sum_j\sum_{i'}\sum_{j'}\sum_{\mathbf{g}}\sum_{\mathbf{h}}\sum_{\mathbf{g}'}\sum_{\mathbf{h}'}\{\text{Bloch waves}\} \times S(\mathbf{Q},\mathbf{Q}')\ \{\text{thickness}\}, \quad (15a)$$

where

$$\{\text{Bloch waves}\} = \alpha_i(-\mathbf{K})\alpha_j^*(-\mathbf{K})\alpha_{i'}(\mathbf{K}_0)\alpha_{j'}^*(\mathbf{K}_0) \times C_g^{(i)}(-\mathbf{K})C_{\mathbf{h}}^{(j)*}(-\mathbf{K})C_{\mathbf{g}'}^{(i')}(\mathbf{K}_0)C_{\mathbf{h}'}^{(j')*}(\mathbf{K}_0), \quad (15b)$$

$$\{\text{thickness}\} = \frac{\{\exp[2\pi i(Q_z + g_z + g_z' + v_i + v_{i'})d] - 1\}}{4\pi^2(Q_z + g_z + g_z' + v_i + v_{i'})} \times \frac{\{\exp[-2\pi i(Q_z' + h_z + h_z' + v_j + v_{j'})d] - 1\}}{(Q_z' + h_z + h_z' + v_j + v_{j'})}, \quad (15c)$$

$$\mathbf{Q}_b = \mathbf{u}_b - \mathbf{g}_b - \mathbf{g}_b', \quad (15d)$$

$$\mathbf{Q}_b' = \mathbf{u}_b - \mathbf{h}_b - \mathbf{h}_b', \quad (15e)$$

$\mathbf{K} = \mathbf{K}_0 + \mathbf{u}_b$, $\mathbf{g}$ and $\mathbf{h}$ are reciprocal-lattice vectors, the subscript b's represent the components parallel to the xy plane and d is the specimen thickness. The sums of i, j, i' and j' are over all the Bloch waves and the sums of $\mathbf{g}$, $\mathbf{h}$, $\mathbf{g}'$ and $\mathbf{h}'$ are over all the reciprocal-lattice vectors. In (15*a*), the {Bloch waves} term characterizes the dynamical diffraction before and after diffuse scattering; S is responsible for the electron angular distribution due to diffuse scattering alone. Equations (15*d*) and (15*e*) are the results of momentum conservation parallel to the surface of the thin slab. The {Bloch waves} term will be modified if the absorption potential is included [see (57)]. Based on these discussions, diffuse scattering due to both TDS and SRO of defects can be calculated using the available theoretical approaches, provided the dynamic form factor $S(\mathbf{Q}, \mathbf{Q}')$ is known.

4. Calculations of dynamic form factors

4.1. *SRO of point vacancies*

The distribution of point vacancies varies from cell to cell. Therefore, a statistical structural average on different cell configurations must be made in the calculation. For simplicity, we consider a case in which the crystal structure is dominated by a periodic lattice but with some point vacancies (Fig. 5). The positions of the atoms are assumed not to be affected by the point vacancies. Since each atom is also vibrating around its equilibrium position, the instantaneous position of the κth atom site in the crystal is $\mathbf{r}_\kappa' = \mathbf{r}_\kappa + \mathbf{U}_\kappa(t)$, where $\mathbf{U}_\kappa$ is the instantaneous displacement of the atom from its equilibrium position $\mathbf{r}_\kappa$. The calculation can be conveniently performed if the crystal potential is expressed as a Fourier transform of the scattering factors $[f_\kappa^e(\boldsymbol{\tau})]$:

$$V(\mathbf{r}, t) = \sum_\kappa \sigma_\kappa V_\kappa(\mathbf{r} - \mathbf{r}_\kappa') = \sum_\kappa \int d\boldsymbol{\tau} \exp[2\pi i(\mathbf{r} - \mathbf{r}_\kappa - \mathbf{U}_\kappa)\cdot\boldsymbol{\tau}]\ \sigma_\kappa f_\kappa^e(\boldsymbol{\tau}), \quad (16)$$

with operator $\sigma_\kappa = 1$ if the site is occupied and $\sigma_\kappa(x) = 0$ if the site is vacant. The structure average is to effectively reduce the scattering power of each atom, thus,

$$V_0(\mathbf{r}) = \chi_0 \sum_\kappa \int d\boldsymbol{\tau} \exp[2\pi i(\mathbf{r} - \mathbf{r}_\kappa)\cdot\boldsymbol{\tau}]\ f_\kappa^e(\boldsymbol{\tau}) \exp[-W_\kappa(\boldsymbol{\tau})], \quad (17)$$

where $\chi_0 = \langle\sigma_\kappa\rangle_s = 1 - \chi_v$ and χ_v is the probability that a site is vacant, *i.e.* the average density of vacancies in the crystal; χ_0 can be understood as the probability that a site is filled by an atom; a relation of $\langle\exp(X)\rangle_t = \exp(\frac{1}{2}\langle X^2\rangle_t)$ with $\langle X\rangle_t = 0$ was used and $W_\kappa(\boldsymbol{\tau}) = 2\pi^2\langle(\mathbf{U}_\kappa\cdot\boldsymbol{\tau})^2\rangle$ is the Debye–Waller factor. Thus, the deviation potential is

$$\Delta V(\mathbf{r}_1, t) = \sum_\kappa \int d\boldsymbol{\tau} \exp[2\pi i(\mathbf{r}_1 - \mathbf{r}_\kappa)\cdot\boldsymbol{\tau}]\ f_\kappa^e(\boldsymbol{\tau}) \times \{\sigma_\kappa \exp(-2\pi i\mathbf{U}_\kappa\cdot\boldsymbol{\tau}) - \chi_0 \exp[-W_\kappa(\boldsymbol{\tau})]\}. \quad (18)$$

We now calculate the function

$$\langle\Delta V(\mathbf{r}_1, t)\Delta V^*(\mathbf{r}_2, t)\rangle_{ts} = \sum_\kappa\sum_{\kappa'} \int d\boldsymbol{\tau} \int d\mathbf{u} \exp[2\pi i(\mathbf{r}_1 - \mathbf{r}_\kappa)\cdot\boldsymbol{\tau}] \times \exp[-2\pi i(\mathbf{r}_2 - \mathbf{r}_{\kappa'})\cdot\mathbf{u}]\ f_\kappa^e(\boldsymbol{\tau})[f_{\kappa'}^e(\mathbf{u})]^* \times \{\langle\sigma_\kappa\sigma_{\kappa'}\rangle_s\langle\exp[2\pi i(\mathbf{U}_{\kappa'}\cdot\mathbf{u} - \mathbf{U}_\kappa\cdot\boldsymbol{\tau})]\rangle_t - \chi_0^2\exp[-W_\kappa(\boldsymbol{\tau}) - W_{\kappa'}(\mathbf{u})]\}. \quad (19)$$

In comparison to (11), the dynamic form factor is

$$S(\boldsymbol{\tau}, \mathbf{u}) = \sum_\kappa\sum_{\kappa'} \exp[2\pi i(\mathbf{r}_{\kappa'}\cdot\mathbf{u} - \mathbf{r}_\kappa\cdot\boldsymbol{\tau})]\ f_\kappa^e(\boldsymbol{\tau})[f_{\kappa'}^e(\mathbf{u})]^* \times \exp[-W_\kappa(\boldsymbol{\tau}) - W_{\kappa'}(\mathbf{u})] \times \{\langle\sigma_\kappa\sigma_{\kappa'}\rangle_s \exp[2F_{\kappa\kappa'}(\boldsymbol{\tau}, \mathbf{u})] - \chi_0^2\}, \quad (20)$$

where

$$F_{\kappa\kappa'}(\boldsymbol{\tau}, \mathbf{u}) = 2\pi^2\langle(\mathbf{U}_\kappa\cdot\boldsymbol{\tau})(\mathbf{U}_{\kappa'}\cdot\mathbf{u})\rangle_t \quad (21)$$

is defined as a correlation function that is related to the coupling between atom vibrations (Wang, 1995*b*). Equation (20) includes not only the diffuse scattering produced by point vacancies but also that due to TDS. The structure and time averages can be performed individually.

Based on the harmonic oscillators and adiabatic approximations, in which all the atoms are assumed to interact with harmonic forces and the crystal electrons move as though the ions were fixed in their instantaneous positions, the correlation function $F_{\kappa\kappa'}(\boldsymbol{\tau}, \mathbf{u})$ has

been calculated analytically using the Warren (1990) approximation (Wang, 1995*a*,*b*). In this approximation, all vibration waves can be considered as either pure longitudinal or pure transverse; the velocities of all longitudinal waves are replaced by an average longitudinal velocity and the velocities of all transverse waves by an average transverse velocity; each average velocity is considered to be a constant independent of the phonon wave vector **q**, the Brillouin zone is replaced by a sphere of radius q_m, whose volume is equal to that of the Brillouin zone. The result gives a criterion for determining the coherent property of the diffuse scattering waves generated within a local region. In general, the coherent length is approximately 1 nm, about 4–5 interatomic distances. If two atoms are separated by more than 1 nm, the TDS waves generated from the two atom sites are incoherent.

We now consider the statistical structure average of $\langle\sigma_\kappa\sigma_{\kappa'}\rangle_s$. With the Flinn symbols (Flinn, 1956),

$$\delta\sigma_\kappa = \sigma_\kappa - \chi_0 = \chi_v - \sigma_\kappa^v, \tag{22}$$

where σ_κ^v is a vacancy operator with $\sigma_\kappa^v = 0$ if the site is occupied and $\sigma_\kappa^v = 1$ if the site is vacant, then

$$\begin{aligned}\langle\sigma_\kappa\sigma_{\kappa'}\rangle_s &= \langle[\delta\sigma_\kappa + \chi_0][\delta\sigma_{\kappa'} + \chi_0]\rangle_s \\ &= \langle\delta\sigma_\kappa\delta\sigma_{\kappa'}\rangle_s + \chi_0^2.\end{aligned} \tag{23}$$

If the interatomic distance between the κ and κ' atoms is denoted as $\mathbf{r}_{\kappa\kappa'} = \mathbf{r}_\kappa - \mathbf{r}_{\kappa'}$, $\langle\delta\sigma_\kappa\delta\sigma_{\kappa'}\rangle_s$ is directly related to the Cowley short-range order (SRO) parameters (Cowley, 1950) defined by

$$\alpha_{\kappa\kappa'} = \langle\delta\sigma_\kappa\delta\sigma_{\kappa'}\rangle_s/\chi_0\chi_v \tag{24}$$

with $\alpha_{\kappa\kappa} = 1$. In kinematical scattering theory, the SRO parameters are the Fourier coefficients of the diffuse scattering intensity distribution (De Ridder, Van Tendeloo & Amelinckx, 1976). This is the principle of using the experimentally measured I_D to calculate SRO parameters (Dai, Wang & Liu, 1996). To show the physical meaning of SRO parameters, we now examine the relationship between $\langle\delta\sigma_\kappa\delta\sigma_{\kappa'}\rangle_s$ and the correlation probability. From (22), the probability of finding a vacancy at a given distance $\mathbf{r}_{\kappa\kappa'}$ ($\kappa \neq \kappa'$) from another vacancy at site κ is

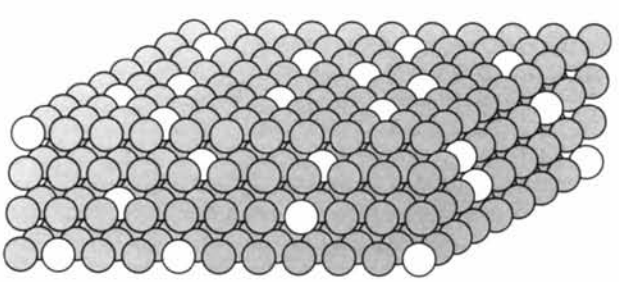

Fig. 5. A schematic model showing point vacancies in a crystal. The shadowed spheres are atoms and the open circles represent point vacancies.

$$\begin{aligned}P_{\kappa\kappa'}^{vv} = \langle\sigma_\kappa^v\sigma_{\kappa'}^v\rangle_s &= \langle(\chi_v - \delta\sigma_\kappa)(\chi_v - \delta\sigma_{\kappa'})\rangle_s \\ &= \chi_v^2 + \langle\delta\sigma_\kappa\delta\sigma_{\kappa'}\rangle_s \\ &= \chi_v^2 + \chi_0\chi_v\alpha_{\kappa\kappa'},\end{aligned} \tag{25}$$

where the first term χ_v^2 represents the probability of two vacancies distributed at κ and κ' if there is no correlation (*i.e.* random distribution). Each vacancy site is a point defect (see Fig. 3*a*). By the same token, the probability of finding an atom at a given distance $(\mathbf{r}_\kappa - \mathbf{r}_{\kappa'})$ from an atom at site κ' is

$$P_{\kappa\kappa'}^{aa} = \langle\sigma_\kappa^a\sigma_{\kappa'}^a\rangle = \chi_0^2 + \chi_0\chi_v\alpha_{\kappa\kappa'}. \tag{26}$$

The probability of finding a vacancy at a given distance $(\mathbf{r}_\kappa - \mathbf{r}_{\kappa'})$ from another atom at site κ' is

$$\begin{aligned}P_{\kappa\kappa'}^{va} = \langle\sigma_\kappa^v\sigma_{\kappa'}^a\rangle &= \langle(\chi_v - \delta\sigma_\kappa)(\chi_0 + \delta\sigma_{\kappa'})\rangle_s \\ &= \chi_v\chi_0 - \langle\delta\sigma_k\delta\sigma_{k'}\rangle_s \\ &= \chi_v\chi_0 - \chi_0\chi_v\alpha_{\kappa\kappa'},\end{aligned} \tag{27}$$

where the first term $\chi_v\chi_0$ is the probability of finding a vacancy at site κ and an atom at site κ' if there is no preferred distribution. The whole set of correlation parameters, for all numbers of atoms, can be considered to specify the state of order of the system. The values of $\alpha_{\kappa\kappa'}$ specify the degree to which the neighbors of one sort of atom tend to be preferably of the same sort or of the opposite sort. If $\alpha_{\kappa\kappa'}$ is positive, $P_{\kappa\kappa'}^{vv} > \chi_v^2$, $P_{\kappa\kappa'}^{aa} > \chi_0^2$, the vacancies tend to clump together with vacancies and atoms tend to clump with atoms. If $\alpha_{\kappa\kappa'}$ is negative, $P_{\kappa\kappa'}^{vv} < \chi_v^2$, $P_{\kappa\kappa'}^{av} > \chi_v\chi_0$, the vacancies tend to clump together with atoms. Therefore, the measurement of $\alpha_{\kappa\kappa'}$ can reflect the short-range order in the considered system. The decrease of $\alpha_{\kappa\kappa'}$ with the increase of $\mathbf{r}_{\kappa\kappa'}$ gives the range of order.

The dynamic form factor given in (20) can be written as

$$\begin{aligned}S(\mathbf{Q}, \mathbf{Q}') = \sum_\kappa\sum_{\kappa'} &\exp[2\pi i(\mathbf{r}_{\kappa'}\cdot\mathbf{Q}' - \mathbf{r}_\kappa\cdot\mathbf{Q})]\, f_\kappa^e(\mathbf{Q}) \\ &\times [f_\kappa^e(\mathbf{Q}')]^* \exp[-W_\kappa(\mathbf{Q}) - W_{\kappa'}(\mathbf{Q}')] \\ &\times \{\chi_0\chi_v\alpha_{\kappa\kappa'}\exp[2F_{\kappa\kappa'}(\mathbf{Q}, \mathbf{Q}')] \\ &+ \chi_0^2\{\exp[2F_{\kappa\kappa'}(\mathbf{Q}, \mathbf{Q}')] - 1\}\}.\end{aligned} \tag{28}$$

This equation covers the diffuse scattering produced by thermal vibration and SRO of point vacancies. The first term in $\{\}$ is due to point vacancies and the second term is due to TDS. The key in the calculation of (28) is the SRO parameters. In the case of SRO in ZrO_2 (Fig. 2), the $\alpha_{\kappa\kappa'}$ parameters have been calculated from the experimental diffraction patterns based on kinematical electron diffraction theory (Dai, Wang & Liu, 1996). These parameters can be used in dynamical calculation to quantitatively fit the experimental data.

If there is no order in the distribution of point vacancies, *i.e.* $\alpha_{\kappa\kappa'} = \delta_{\kappa\kappa'}$, and with the use of the Einstein model, (28) is approximated as

$$S(\mathbf{Q},\mathbf{Q}') = \sum_{\kappa} \exp[2\pi i \mathbf{r}_\kappa \cdot (\mathbf{Q}' - \mathbf{Q})]\, f_\kappa^e(\mathbf{Q})[f_\kappa^e(\mathbf{Q}')]^* \times \{\chi_0 \exp[-W_\kappa(\mathbf{Q} - \mathbf{Q}')] - \chi_0^2 \exp[-W_\kappa(\mathbf{Q}) - W_\kappa(\mathbf{Q}')]\}. \quad (29)$$

This is just the result obtained by Dudarev, Vvedensky & Whelan (1993). Equation (29) can be further simplified if the position of the κth atom is a sum of the unit-cell position $\mathbf{R}_n$ and the relative position $\mathbf{r}(\beta)$ of the atom with respect to the origin of the unit cell, *i.e.* $\mathbf{r}_\kappa = \mathbf{R}_n + \mathbf{r}(\beta)$,

$$S(\mathbf{Q},\mathbf{Q}') = \sum_{\mathbf{g}''} \delta(\mathbf{Q}' - \mathbf{Q} - \mathbf{g}'') \Big\{ \sum_{\beta} \exp[2\pi i \mathbf{r}(\beta)\cdot\mathbf{g}''] \times f_\beta^e(\mathbf{Q})[f_\beta^e(\mathbf{Q}+\mathbf{g}'')]^* \{\chi_0 \exp[-W_\beta(\mathbf{g}'')] - \chi_0^2 \exp[-W_\beta(\mathbf{Q}) - W_\beta(\mathbf{Q}+\mathbf{g}'')]\} \Big\}, \quad (30)$$

where an identity $\sum_n \exp[2\pi i \mathbf{R}_n \cdot \mathbf{u}] = \sum_{\mathbf{g}''} \delta(\mathbf{u} - \mathbf{g}'')$ for a periodic structure was used and $\mathbf{g}''$ are reciprocal-lattice vectors.

4.2. *Atom substitution in a binary alloy system*

A classical example in SRO is a simple binary alloy solution, composed of A and B types of atoms with fractional proportions χ_A and χ_B, such as Cu_3Au and CuAu (Fig. 6). These alloys usually have a simple cubic structure. In this section, we calculate the dynamic form factor for this system where the atom substitution can occur. For simplicity, we consider a crystal containing two types of atom. The extension to systems with more than two types of atom follows with elaboration of the algebra but little difference in conception. The ordering in the crystal is defined by order parameters that define correlation between the occupancy of sites, which, for example, is the probability $P_{\kappa\kappa'}^{AB}$ of finding a B atom (at site κ') at a given position $(\mathbf{r}_{\kappa'} - \mathbf{r}'_\kappa)$ from an A atom at site κ. To describe the potential distribution in this system, we first introduce the occupation operators (Flinn, 1956; Cowley, 1995):

$$\sigma_\kappa^A = \begin{cases} 1 & \text{for an } A \text{ atom at site } \kappa \\ 0 & \text{for a } B \text{ atom at site } \kappa \end{cases} \quad (31a)$$

and

$$\sigma_\kappa^B = \begin{cases} 1 & \text{for a } B \text{ atom at site } \kappa \\ 0 & \text{for an } A \text{ atom at site } \kappa. \end{cases} \quad (31b)$$

These parameters are interconnected and we may replace both by a single parameter

$$\delta\sigma_\kappa = \begin{cases} \chi_B & \text{for an } A \text{ atom at site } \kappa \\ -\chi_A & \text{for a } B \text{ atom at site } \kappa. \end{cases} \quad (32)$$

Thus,

$$\delta\sigma_\kappa = \sigma_\kappa^A - \chi_A = \chi_B - \sigma_\kappa^B \quad (33)$$

with $\langle\delta\sigma_\kappa\rangle_s = 0$ and $\chi_A + \chi_B = 1$. The probability is given by

$$P_{\kappa\kappa'}^{AB} = \langle\sigma_\kappa^A\sigma_{\kappa'}^B\rangle = \chi_A\chi_B - \langle\delta\sigma_\kappa\delta\sigma_{\kappa'}\rangle_s. \quad (34a)$$

Similarly,

$$P_{\kappa\kappa'}^{AA} = \langle\sigma_\kappa^A\sigma_{\kappa'}^A\rangle = \chi_A^2 + \langle\delta\sigma_\kappa\delta\sigma_{\kappa'}\rangle_s. \quad (34b)$$

The Cowley SRO parameters are defined by

$$\alpha_{\kappa\kappa'} = \langle\delta\sigma_\kappa\delta\sigma_{\kappa'}\rangle_s/\chi_A\chi_B. \quad (35)$$

If $\alpha_{\kappa\kappa'}$ is positive, $P_{\kappa\kappa'}^{AA} > \chi_A^2$, $P_{\kappa\kappa'}^{AB} < \chi_A\chi_B$, the same types of atom tend to clump together. If $\alpha_{\kappa\kappa'}$ is negative, $P_{\kappa\kappa'}^{AA} < \chi_A^2$, $P_{\kappa\kappa'}^{AB} > \chi_A\chi_B$, the A atoms tend to clump with B atoms.

After defining these SRO parameters, we now consider the crystal potential distribution with the presence of lattice substitution between the A and B atoms. If the thermal vibrations of crystal atoms are also considered, the instantaneous position of the κth atom in the crystal is $\mathbf{r}'_\kappa = \mathbf{r}_\kappa + \mathbf{U}_\kappa(t)$, where $\mathbf{U}_\kappa$ is the instantaneous displacement of the atom from its equilibrium position $\mathbf{r}_\kappa$. We assume that the lattice position $\mathbf{r}_\kappa$ is not affected by the atom substitution, *i.e.* lattice relaxation caused by the atom size effect is ignored. The crystal potential may be written as

$$V(\mathbf{r},t) = \sum_\kappa [\sigma_\kappa^A V_A(\mathbf{r} - \mathbf{r}_\kappa - \mathbf{U}_\kappa^A) + \sigma_\kappa^B V_B(\mathbf{r} - \mathbf{r}_\kappa - \mathbf{U}_\kappa^B)] = \sum_\kappa \int d\boldsymbol{\tau} \exp[2\pi i(\mathbf{r} - \mathbf{r}_\kappa)\cdot\boldsymbol{\tau}] \times [\sigma_\kappa^A f_A^e(\boldsymbol{\tau}) \exp(-2\pi i \mathbf{U}_\kappa^A\cdot\boldsymbol{\tau}) + \sigma_\kappa^B f_B^e(\boldsymbol{\tau}) \exp(-2\pi i \mathbf{U}_\kappa^B\cdot\boldsymbol{\tau})], \quad (36)$$

where $\mathbf{U}_\kappa^A$ (or $\mathbf{U}_\kappa^B$) stands for the vibration displacement of the A (or B atom) located at site κ. The time and structure averages are to effectively reduce the scattering power of each atom, thus,

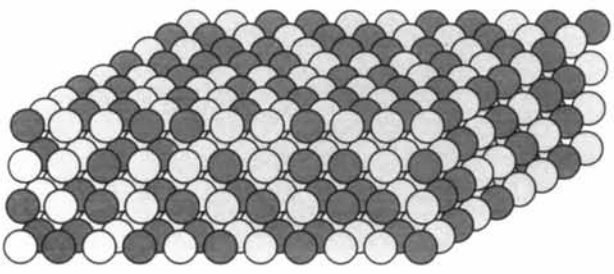

Fig. 6. A schematic model showing atom substitution in a binary crystal.

$$V_0(\mathbf{r}) = \langle V(\mathbf{r}, t)\rangle_{ts} = \sum_{\kappa} \int d\boldsymbol{\tau} \exp[2\pi i(\mathbf{r} - \mathbf{r}_\kappa)\cdot\boldsymbol{\tau}] \times \{\chi_A f_A^e(\boldsymbol{\tau}) \exp[-W_\kappa^A(\boldsymbol{\tau})] + \chi_B f_B^e(\boldsymbol{\tau}) \exp[-W_\kappa^B(\boldsymbol{\tau})]\}, \tag{37}$$

where $W_\kappa^A(\boldsymbol{\tau})$ [or $W_\kappa^B(\boldsymbol{\tau})$] stands for the Debye-Waller factor of the A (or B) atom located at site κ. The deviation potential is

$$\Delta V(\mathbf{r}_1, t) = \sum_{\kappa} \int d\boldsymbol{\tau} \exp[2\pi i(\mathbf{r}_1 - \mathbf{r}_\kappa)\cdot\boldsymbol{\tau}] \times \Big(f_A^e(\boldsymbol{\tau})\{\sigma_\kappa^A \exp(-2\pi i \mathbf{U}_\kappa^A\cdot\boldsymbol{\tau}) - \chi_A \exp[-W_\kappa^A(\boldsymbol{\tau})]\} + f_B^e(\boldsymbol{\tau})\{\sigma_\kappa^B \exp(-2\pi i \mathbf{U}_\kappa^B\cdot\boldsymbol{\tau}) - \chi_B \exp[-W_\kappa^B(\boldsymbol{\tau})]\}\Big). \tag{38}$$

We now calculate the function

$$\begin{aligned}\langle \Delta V(\mathbf{r}_1, t)\Delta V^*(\mathbf{r}_2, t)\rangle_{ts} &= \sum_{\kappa}\sum_{\kappa'} \int d\boldsymbol{\tau} \int d\mathbf{u} \exp[2\pi i(\mathbf{r}_1 - \mathbf{r}_\kappa)\cdot\boldsymbol{\tau}] \times \exp[-2\pi i(\mathbf{r}_2 - \mathbf{r}_{\kappa'})\cdot\mathbf{u}] \\ &\times \Big\langle \Big(f_A^e(\boldsymbol{\tau})\{\sigma_\kappa^A \exp(-2\pi i \mathbf{U}_\kappa^A\cdot\boldsymbol{\tau}) - \chi_A \exp[-W_\kappa^A(\boldsymbol{\tau})]\} \\ &+ f_B^e(\boldsymbol{\tau})\{\sigma_\kappa^B \exp(-2\pi i \mathbf{U}_\kappa^B\cdot\boldsymbol{\tau}) - \chi_B \exp[-W_\kappa^B(\boldsymbol{\tau})]\}\Big) \\ &\times \Big([f_A^e(\mathbf{u})]^*\{\sigma_{\kappa'}^A \exp(2\pi i \mathbf{U}_{\kappa'}^A\cdot\mathbf{u}) - \chi_A \exp[-W_{\kappa'}^A(\mathbf{u})]\} \\ &+ [f_B^e(\mathbf{u})]^*\{\sigma_{\kappa'}^B \exp(2\pi i \mathbf{U}_{\kappa'}^B\cdot\mathbf{u}) \\ &- \chi_B \exp[-W_{\kappa'}^B(\mathbf{u})]\}\Big)\Big\rangle_{ts}. \end{aligned} \tag{39}$$

The statistical structure average can be performed using following relations:

$$\langle \sigma_\kappa^A \sigma_{\kappa'}^A\rangle_s = \langle(\chi_A + \delta\sigma_\kappa)(\chi_A + \delta\sigma_{\kappa'})\rangle_s = \chi_A^2 + \langle\delta\sigma_\kappa\delta\sigma_{\kappa'}\rangle = \chi_A^2 + \chi_A\chi_B\alpha_{\kappa\kappa'}, \tag{40a}$$

$$\langle \sigma_\kappa^B \sigma_{\kappa'}^A\rangle_s = \langle(\chi_B - \delta\sigma_\kappa)(\chi_A + \delta\sigma_{\kappa'})\rangle_s = \chi_A\chi_B - \langle\delta\sigma_\kappa\delta\sigma_{\kappa'}\rangle = \chi_A\chi_B - \chi_A\chi_B\alpha_{\kappa\kappa'}, \tag{40b}$$

$$\langle \sigma_\kappa^A \sigma_{\kappa'}^B\rangle_s = \langle(\chi_A + \delta\sigma_\kappa)(\chi_B - \delta\sigma_{\kappa'})\rangle_s = \chi_A\chi_B - \langle\delta\sigma_\kappa\delta\sigma_{\kappa'}\rangle = \chi_A\chi_B - \chi_A\chi_B\alpha_{\kappa\kappa'} \tag{40c}$$

and

$$\langle \sigma_\kappa^B \sigma_{\kappa'}^B\rangle_s = \langle(\chi_B - \delta\sigma_\kappa)(\chi_B - \delta\sigma_{\kappa'})\rangle_s = \chi_B^2 + \langle\delta\sigma_\kappa\delta\sigma_{\kappa'}\rangle = \chi_B^2 + \chi_A\chi_B\alpha_{\kappa\kappa'}. \tag{40d}$$

In reference to the dynamic form factor defined in (11), one has

$$\begin{aligned} S(\boldsymbol{\tau}, \mathbf{u}) = \sum_{\kappa}\sum_{\kappa'} \exp[-2\pi i(\mathbf{r}_\kappa\cdot\boldsymbol{\tau} - \mathbf{r}_{\kappa'}\cdot\mathbf{u})] &\times \Big(f_A^e(\boldsymbol{\tau})[f_A^e(\mathbf{u})]^* \exp[-W_\kappa^A(\boldsymbol{\tau}) - W_{\kappa'}^A(\mathbf{u})] \\ &\times \{(\chi_A^2 + \chi_A\chi_B\alpha_{\kappa\kappa'})\exp[2F_{\kappa\kappa'}^{AA}(\boldsymbol{\tau}, \mathbf{u})] - \chi_A^2\} \\ &+ f_B^e(\boldsymbol{\tau})[f_A^e(\mathbf{u})]^* \exp[-W_\kappa^B(\boldsymbol{\tau}) - W_{\kappa'}^A(\mathbf{u})] \\ &\times \{\chi_A\chi_B(1 - \alpha_{\kappa\kappa'})\exp[2F_{\kappa\kappa'}^{BA}(\boldsymbol{\tau}, \mathbf{u})] - \chi_A\chi_B\} \\ &+ f_A^e(\boldsymbol{\tau})[f_B^e(\mathbf{u})]^* \exp[-W_\kappa^A(\boldsymbol{\tau}) - W_{\kappa'}^B(\mathbf{u})] \\ &\times \{\chi_A\chi_B(1 - \alpha_{\kappa\kappa'})\exp[2F_{\kappa\kappa'}^{AB}(\boldsymbol{\tau}, \mathbf{u})] - \chi_A\chi_B\} \\ &+ f_B^e(\boldsymbol{\tau})[f_B^e(\mathbf{u})]^* \exp[-W_\kappa^B(\boldsymbol{\tau}) - W_{\kappa'}^B(\mathbf{u})] \\ &\times \{(\chi_B^2 + \chi_A\chi_B\alpha_{\kappa\kappa'})\exp[2F_{\kappa\kappa'}^{BB}(\boldsymbol{\tau}, \mathbf{u})] - \chi_B^2\}\Big), \end{aligned} \tag{41}$$

where $F_{\kappa\kappa'}^{ab}(\boldsymbol{\tau}, \mathbf{u}) = 2\pi^2\langle[(\mathbf{U}_\kappa^a\cdot\boldsymbol{\tau})(\mathbf{U}_{\kappa'}^b\cdot\mathbf{u})]\rangle_t$ is the correlation function between a and b atoms located at sites κ and κ', respectively, and it has been calculated using the Warren approximation (Wang, 1995*a*).

If the site substitution is random, so that $\alpha_{\kappa\kappa'} = \delta_{\kappa\kappa'}$, and if the Einstein model is also used for thermal vibration, one has

$$\begin{aligned} S(\boldsymbol{\tau}, \mathbf{u}) = \sum_{\kappa} \exp[-2\pi i\mathbf{r}_\kappa\cdot(\boldsymbol{\tau} - \mathbf{u})] &\times \Big(f_A^e(\boldsymbol{\tau})[f_A^e(\mathbf{u})]^*\{\chi_A \exp[-W_\kappa^A(\boldsymbol{\tau} - \mathbf{u})] \\ &- \chi_A^2 \exp[-W_\kappa^A(\boldsymbol{\tau}) - W_\kappa^A(\mathbf{u})]\} \\ &- \chi_A\chi_B\{f_B^e(\boldsymbol{\tau})[f_A^e(\mathbf{u})]^* + f_A^e(\boldsymbol{\tau})[f_B^e(\mathbf{u})]^*\} \\ &\times \exp[-W_\kappa^B(\boldsymbol{\tau}) - W_\kappa^A(\mathbf{u})] \\ &+ f_B^e(\boldsymbol{\tau})[f_B^e(\mathbf{u})]^*\{\chi_B \exp[-W_\kappa^B(\boldsymbol{\tau} - \mathbf{u})] \\ &- \chi_B^2 \exp[-W_\kappa^B(\boldsymbol{\tau}) - W_\kappa^B(\mathbf{u})]\}\Big). \end{aligned} \tag{42}$$

Using the same procedure as for deriving (30), (42) can be rewritten as

$$\begin{aligned} S(\boldsymbol{\tau}, \mathbf{u}) = \sum_{\mathbf{g}''} \delta(\boldsymbol{\tau} - \mathbf{u} - \mathbf{g}'')\Big[\sum_{\beta} \exp[2\pi i\mathbf{r}(\beta)\cdot\mathbf{g}''] &\times \Big(f_A^e(\boldsymbol{\tau})[f_A^e(\mathbf{u})]^*\{\chi_A \exp[-W_\beta^A(\mathbf{g}'')] \\ &- \chi_A^2 \exp[-W_\beta^A(\boldsymbol{\tau}) - W_\beta^A(\mathbf{u})]\} \\ &- \chi_A\chi_B\{f_B^e(\boldsymbol{\tau})[f_A^e(\mathbf{u})]^* + f_A^e(\boldsymbol{\tau})[f_B^e(\mathbf{u})]^*\} \\ &\times \exp[-W_\beta^B(\boldsymbol{\tau}) - W_\beta^A(\mathbf{u})] + f_B^e(\boldsymbol{\tau})[f_B^e(\mathbf{u})]^* \\ &\times \{\chi_B \exp[-W_\beta^B(\mathbf{g}'')] \\ &- \chi_B^2 \exp[-W_\beta^B(\boldsymbol{\tau}) - W_\beta^B(\mathbf{u})]\}\Big)\Big]. \end{aligned} \tag{43}$$

To check the consistency of (42) with other results, we now consider three extreme cases.

Case 1: If there is no atom substitution, so that $\chi_B = 0$ and $\chi_A = 1$,

$$S(\boldsymbol{\tau}, \mathbf{u}) = \sum_{\kappa} \exp[-2\pi i \mathbf{r}_{\kappa} \cdot (\boldsymbol{\tau} - \mathbf{u})] f_A^e(\boldsymbol{\tau})[f_A^e(\mathbf{u})]^* \times \Big(\exp[-W_{\kappa}^A(\boldsymbol{\tau} - \mathbf{u})] - \exp[-W_{\kappa}^A(\boldsymbol{\tau}) - W_{\kappa}^A(\mathbf{u})] \Big) \quad (44)$$

This is just the dynamic form factor for TDS in the Einstein model.

Case 2: If there were no atom vibration at $T = 0$, so that $W_{\kappa}^A = W_{\kappa}^B = 0$,

$$S(\boldsymbol{\tau}, \mathbf{u}) = \chi_A \chi_B \sum_{\mathbf{g}''} \delta(\boldsymbol{\tau} - \mathbf{u} - \mathbf{g}'')] \Big\{ \sum_{\beta} \exp[2\pi i \mathbf{r}(\beta) \cdot \mathbf{g}''] \times [f_A^e(\boldsymbol{\tau}) - f_B^e(\boldsymbol{\tau})][f_A^e(\mathbf{u}) - f_B^e(\mathbf{u})]^* \Big\}. \quad (45)$$

Thus, the diffuse scattering is caused by the difference in scattering factors of the A and B types of atom.

Case 3: If the A and B atoms are the same element, replacing B and A (and $\chi_A = \chi_B = 1/2$) makes (42) become

$$S(\boldsymbol{\tau}, \mathbf{u}) = \sum_{\kappa} \exp[-2\pi i \mathbf{r}_{\kappa} \cdot (\boldsymbol{\tau} - \mathbf{u})] f_A^e(\boldsymbol{\tau})[f_A^e(\mathbf{u})]^* \times \{\exp[-W_{\kappa}^A(\boldsymbol{\tau} - \mathbf{u})] - \exp[-W_{\kappa}^A(\boldsymbol{\tau}) - W_{\kappa}^A(\mathbf{u})]\}. \quad (46)$$

This equation is identical to (44) for TDS and the SRO effect disappears, just as expected.

It must be pointed out that the calculation of dynamic form factor in this section was performed with the important assumption that the equilibrium position vectors $\mathbf{r}_{\kappa}$ were the same as for a perfect crystal without defects, *i.e.* the lattice relaxation caused by point defects was ignored. The relaxation effect can be reasonably taken into account using the results of Hall (1965). If there is no correlation between point defects, the relaxation effect is equivalent to introducing a similar quantity to the Debye–Waller factor that depends on the average displacement of an atom as a result of lattice relaxation. Thus, the Debye–Waller factor $W_{\kappa}(\mathbf{Q})$ is replaced by $[W_{\kappa}(\mathbf{Q}) + W_{\kappa}^{(d)}(\mathbf{Q})]$, where $W_{\kappa}^{(d)}(\mathbf{Q}) = 2\pi^2 Q^2 \langle v^2 \rangle$ and $\langle v^2 \rangle$ is the mean square displacement produced by lattice relaxation, the calculation of which can be made based on the random-walk model.

5. The 'absorption potential' and multiple diffuse scattering

Since our calculation is made based on the first-order diffuse scattering approximation, *i.e.* $\Psi(\mathbf{r}_1, t)$ is replaced by $\Psi_0(\mathbf{K}_0, \mathbf{r}_1)$ in (3), which is

$$\Psi(\mathbf{r}, t) \simeq \Psi_0(\mathbf{K}_0, \mathbf{r}) + \int d\mathbf{r}_1 G(\mathbf{r}, \mathbf{r}_1)[e\gamma \Delta V(\mathbf{r}_1, t)\Psi_0(\mathbf{K}_0, \mathbf{r}_1)], \quad (47)$$

where the higher-order diffuse scattering terms are dropped. This approximation fails if the specimen is thick and/or the disorder is high. We now modify the solution Ψ_0 of (5) to compensate these high-order diffuse scattering terms so that the theory can be expanded to cases unrestricted by the first-order diffuse scattering approximation. A correction potential $V^{(i)}$ is symbolically introduced,

$$[-(\hbar^2/2m_0)\nabla^2 - e\gamma V_0 - e\gamma V^{(i)} - E]\Psi_0 = 0. \quad (48)$$

The potential $V^{(i)}$ is chosen so that (47) and (48) exactly satisfy the original Schrödinger equation (2) and the result is

$$[V^{(i)}\Psi_0] = e\gamma \int d\mathbf{r}_1 [G(\mathbf{r}, \mathbf{r}_1)\Delta V(\mathbf{r}, t)\Delta V(\mathbf{r}_1, \mathbf{t}) \times \Psi_0(\mathbf{K}_0, \mathbf{r}_1)]. \quad (49)$$

We now prove that the potential $V^{(i)}$ given by (49) can be applied to recover the high-order diffuse scattering terms dropped when $\Psi(\mathbf{r}_1, t)$ is replaced by $\Psi_0(\mathbf{K}_0, \mathbf{r}_1)$ in deriving (8*a*) under the first-order diffuse scattering approximation. Starting from the integral form of (48) and using Green's function and iterative calculation, one can expand the elastic wave as

$$\begin{aligned}
\Psi_0(\mathbf{K}_0, \mathbf{r}) &= \Psi_0^{(0)}(\mathbf{K}_0, \mathbf{r}) \\
&\quad + e\gamma \int d\mathbf{r}_1 G(\mathbf{r}, \mathbf{r}_1)[V^{(i)}(\mathbf{r}_1)\Psi_0(\mathbf{K}_0, \mathbf{r}_1)] \\
&= \Psi_0^{(0)}(\mathbf{K}_0, \mathbf{r}) + (e\gamma)^2 \int d\mathbf{r}_1 G(\mathbf{r}, \mathbf{r}_1) \\
&\quad \times \int d\mathbf{r}_2 [G(\mathbf{r}_1, \mathbf{r}_2)\Delta V(\mathbf{r}_1, t)\Delta V(\mathbf{r}_2, t)\Psi_0(\mathbf{K}_0, \mathbf{r}_2)] \\
&= \Psi_0^{(0)}(\mathbf{K}_0, \mathbf{r}) + (e\gamma)^2 \int d\mathbf{r}_1 \int d\mathbf{r}_2 G(\mathbf{r}, \mathbf{r}_1)G(\mathbf{r}_1, \mathbf{r}_2) \\
&\quad \times \Delta V(\mathbf{r}_1, t)\Delta V(\mathbf{r}_2, t)\Psi_0^{(0)}(\mathbf{K}_0, \mathbf{r}_2) + (e\gamma)^4 \\
&\quad \times \int d\mathbf{r}_1 \int d\mathbf{r}_2 \int d\mathbf{r}_3 \int d\mathbf{r}_4 G(\mathbf{r}, \mathbf{r}_1)G(\mathbf{r}_1, \mathbf{r}_2) \\
&\quad \times G(\mathbf{r}_2, \mathbf{r}_3)G(\mathbf{r}_3, \mathbf{r}_4)\Delta V(\mathbf{r}_1, t)\Delta V(\mathbf{r}_2, t) \\
&\quad \times \Delta V(\mathbf{r}_3, t)\Delta V(\mathbf{r}_4, t)\Psi_0^{(0)}(\mathbf{K}_0, \mathbf{r}_4) + \ldots,
\end{aligned} \quad (50)$$

where $\Psi_0^{(0)}$ is the Bragg scattered wave due to the average periodic lattice at the absence of $V^{(i)}$ (*e.g.* no absorption):

$$[-(\hbar^2/2m_0)\nabla^2 - e\gamma V_0 - E]\Psi_0^{(0)} = 0. \quad (51)$$

This equation can be solved using conventional dynamic electron diffraction theory. Substitution of (50) into (8*a*) gives the total scattered wave:

$$\Psi(\mathbf{r},t)=\Psi_0^{(0)}(\mathbf{K}_0,\mathbf{r})$$
$$+(e\gamma)\int d\mathbf{r}_1 G(\mathbf{r},\mathbf{r}_1)\Delta V(\mathbf{r}_1,t)\Psi_0^{(0)}(\mathbf{K}_0,\mathbf{r}_1)$$
$$+(e\gamma)^2\int d\mathbf{r}_1\int d\mathbf{r}_2 G(\mathbf{r},\mathbf{r}_1)G(\mathbf{r}_1,\mathbf{r}_2)$$
$$\times\Delta V(\mathbf{r}_1,t)\Delta V(\mathbf{r}_2,t)\Psi_0^{(0)}(\mathbf{K}_0,\mathbf{r}_2)$$
$$+(e\gamma)^3\int d\mathbf{r}_1\int d\mathbf{r}_2\int d\mathbf{r}_3 G(\mathbf{r},\mathbf{r}_1)G(\mathbf{r}_1,\mathbf{r}_2)$$
$$\times G(\mathbf{r}_2,\mathbf{r}_3)\Delta V(\mathbf{r}_1,t)\Delta V(\mathbf{r}_2,t)$$
$$\times\Delta V(\mathbf{r}_3,t)\Psi_0^{(0)}(\mathbf{K}_0,\mathbf{r}_3)$$
$$+(e\gamma)^4\int d\mathbf{r}_1\int d\mathbf{r}_2\int d\mathbf{r}_3\int d\mathbf{r}_4 G(\mathbf{r},\mathbf{r}_1)G(\mathbf{r}_1,\mathbf{r}_2)$$
$$\times G(\mathbf{r}_2,\mathbf{r}_3)G(\mathbf{r}_3,\mathbf{r}_4)\Delta V(\mathbf{r}_1,t)\Delta V(\mathbf{r}_2,t)$$
$$\times\Delta V(\mathbf{r}_3,t)\Delta V(\mathbf{r}_4,t)\Psi_0^{(0)}(\mathbf{K}_0,\mathbf{r}_4)+\ldots. \quad (52)$$

This Born series is the exact solution of (2) without making any approximation. The third term in (52) is taken as an example to show its physical meaning, as schematically shown in Fig. 3. The Bragg scattered wave is diffusely scattered at $\mathbf{r}_2$ by $\Delta V(\mathbf{r}_2,t)$. The diffusely scattered wave is elastically scattered by the crystal lattice while propagating from $\mathbf{r}_2$ to $\mathbf{r}_1$ $[G(\mathbf{r}_1,\mathbf{r}_2)]$, then, the second-order diffuse scattering occurs at $\mathbf{r}_1$ $[\Delta V(\mathbf{r}_1,t)]$. Finally, the double diffusely scattered wave exits the crystal at $\mathbf{r}$ after elastic scattering when propagating from $\mathbf{r}_1$ to $\mathbf{r}$ $[G(\mathbf{r},\mathbf{r}_1)]$. The integrals over $\mathbf{r}_1$ and $\mathbf{r}_2$ sum over the contributions made by all of the possible scattering sources in the crystal.

Therefore, the multiple diffusely scattered waves are comprehensively included in the calculation of (8*a*) if the optical potential $V^{(i)}$ given by (49) is introduced in the calculation of Ψ_0 [(48)]. This is a key conclusion, which means that, by introducing a proper form of the optical potential, the multiple diffuse scattering terms are automatically included in the calculation using (8*a*), although it was derived for the first-order diffuse scattering. This result has a strong impact on the conventional diffuse scattering theories developed based on the first-order diffuse scattering. Thus, an introduction of a complex potential $V^{(i)}$ in the calculation of the elastic wave makes the existing theories available for calculating the TDS and SRO including all orders of effects. This conclusion is universal for a time-independent system because no assumption and approximation was made in the proof.

We now modify (15) to make this Bloch-wave theory suitable for calculations beyond the restriction of the first-order diffuse scattering. In practical calculations, a time and structure average is made over (49):

$$[V^{(i)}\Psi_0]=e\gamma\int d\mathbf{r}_1[G(\mathbf{r},\mathbf{r}_1)$$
$$\times\langle\Delta V(\mathbf{r},t)\Delta V(\mathbf{r}_1,t)\rangle_{ts}\Psi_0(\mathbf{K}_0,\mathbf{r}_1)]. \quad (53)$$

A detailed method for the calculation of $V^{(i)}$ for a general case is given elsewhere (Wang, 1996*b*, 1997). For simple illustrational purposes, we make the following approximation. To proceed with the calculation of (53), one ignores the diffraction effect of the crystal so that the Green function is replaced by its free-space form (Yoshioka, 1957):

$$G_0(\mathbf{r},\mathbf{r}_1)\simeq(2m_0/\hbar^2)[\exp(2\pi iK|\mathbf{r}-\mathbf{r}_1|)/4\pi|\mathbf{r}-\mathbf{r}_1|]. \quad (54)$$

With the dynamic form factor introduced in (11), (53) becomes

$$[V^{(i)}\Psi_0]\simeq(m_0e\gamma/2\pi\hbar^2)\int d\mathbf{Q}\int d\mathbf{Q}'S(\mathbf{Q},\mathbf{Q}')$$
$$\times\int d\mathbf{r}_1\{[\exp(2\pi iK|\mathbf{r}-\mathbf{r}_1|)/|\mathbf{r}-\mathbf{r}_1|]$$
$$\times\exp[2\pi i(\mathbf{r}\cdot\mathbf{Q}-\mathbf{r}_1\cdot\mathbf{Q}')]\,\Psi_0(\mathbf{K}_0,\mathbf{r}_1)\}. \quad (55)$$

From (55), the correction potential $V^{(i)}$ is a complex function, its imaginary component denotes the 'absorption' effect. More importantly, this potential is not a local function because $V^{(i)}$ cannot be separated from wave function Ψ_0. The most accurate representation of this non-local imaginary component is to use its Fourier coefficients given in a matrix form; the $(\mathbf{g},\mathbf{h})$ matrix elements are given by (Yoshioka, 1957; Yoshioka & Kainuma, 1962; Wang, 1995*a*)

$$V_{gh}^{(i)}\simeq-(em_0\gamma/2\pi^2\hbar^2V_c)\{\int d\tau(\mathbf{u})$$
$$\times[S(\mathbf{k}_\mathbf{g}-\mathbf{u},\mathbf{k}_\mathbf{h}-\mathbf{u})/(K_0^2-u^2)]$$
$$+i(\pi/2K_0)\int d\sigma(\mathbf{u})\,S(\mathbf{k}_\mathbf{g}-\mathbf{u},\mathbf{k}_\mathbf{h}-\mathbf{u})\}, \quad (56)$$

where V_c is the volume of the crystal, the integral $\tau(\mathbf{u})$ is over all reciprocal space $\mathbf{u}$ except a spherical shell defined by $|\mathbf{u}|=K_0$ and the integral $\sigma(\mathbf{u})$ is on the surface of the Ewald sphere defined by $|\mathbf{u}|=K_0$, with $\mathbf{k}_\mathbf{g}\simeq\mathbf{K}_0+\mathbf{g}$ and $\mathbf{k}_\mathbf{h}\simeq\mathbf{K}_0+\mathbf{h}$. The dynamic form factor S is the most important function in this calculation.

If the Green function G in (52) is replaced by its form in free space (G_0), this means that the dynamical Bragg diffraction of the electrons is ignored after each order of diffuse scattering. Therefore, Yoshioka's approximation of replacing G by G_0 still recovers the multiple diffuse scattering terms but the dynamic diffraction effects after each event, similar to Høier's (1973) multiple inelastic scattering for plasmon excitation. Therefore, the 'absorption potential' has a much richer meaning than the conventional interpretation of an absorption effect. In practical calculations, the real component of $V_{gh}^{(i)}$ may need to be preserved because it may not be small enough for a highly disordered crystal. A detailed application of this result for transmission electron diffraction will be reported separately (Wang, 1996*b*).

Based on the discussion above, we must make the following modifications to the theory presented in §3. Since the reciprocity theorem holds if there is no absorption [*i.e.* (9)] in (12), the calculation of $\Psi_0(-\mathbf{K},\mathbf{r})$ should not include absorption, while the

calculation of $\Psi_0(\mathbf{K}_0, \mathbf{r})$ must include the absorption potential. Accordingly, the {Bloch waves} term in (15*a*) is modified to

$$\{\text{Bloch waves}\} = C_0^{(i)*}(-\mathbf{K})C_0^{(j)}(-\mathbf{K})C_{I'0}^{(i')}(\mathbf{K}_0) \times C_{I'0}^{(j')*}(\mathbf{K}_0)C_{\mathbf{g}}^{(i)}(-\mathbf{K})C_{\mathbf{h}}^{(j)*}(-\mathbf{K}) \times C_{\mathbf{g}'}^{(i')}(\mathbf{K}_0)C_{\mathbf{h}'}^{(j')*}(\mathbf{K}_0), \quad (57)$$

where the $\{C_{\mathbf{g}}\}$ coefficients should be calculated with (14) without consideration of absorption potential $V_{\mathbf{gh}'}$, while the calculations of $\{C_{\mathbf{g}'}\}$ and $\{C_{I'}\}$ need to include the absorption potential [*e.g.* $V_{\mathbf{g}-\mathbf{h}}$ is replaced by $(V_{\mathbf{g}-\mathbf{h}} + V_{\mathbf{gh}'})$ in (14)]. The corrections introduced by the absorption potential on ν_i are ignored.

The absorption potentials introduced by TDS have been calculated by Bird & King (1990) and Allen & Rossouw (1990) using the Einstein model. The absorption potential introduced by point vacancies has been calculated by Dudarev, Peng & Whelan (1992), who showed the significance of the non-local characteristic of the imaginary potential. Therefore, the conventional assumption that $V^{(i)}$ is a fraction of V_0 [*i.e.* $V^{(i)} = AV_0(\mathbf{r})$, with a proportional constant $A \ll 1$] is not adequate.

As a summary, the dynamic form factor is directly related to the SRO parameters. These parameters can either be measured experimentally using X-ray or neutron diffraction or be calculated by Monte Carlo similations. The objective of our dynamical theory is to simulate quantitatively the electron diffraction patterns for deriving the SRO parameters. The calculations using (56) need an accurate representation of the electron scattering factor at large scattering angles. The empirical analytical expression proposed by Weickenmeier & Kohl (1991) is expected to give more accurate results than that given by Doyle & Turner (1968) because special consideration was made at large scattering angles.

6. Conclusions

In this paper, a formal dynamical theory is developed to calculate the diffuse scattering produced by atom vibrations and point defects with short-range order (SRO). Diffuse scattering not only produces fine details in the diffraction pattern between Bragg beams but also introduces an imaginary potential that reduces the intensities of the Bragg reflected beams. The distribution of diffusely scattered electrons and the absorption potential are directly related to a dynamic form factor $S(\mathbf{Q}, \mathbf{Q}')$, which has been described for cases where point vacancies and atom substitutions are present, and the final results are directly related to Cowley's SRO parameters. The equation best suited for numerical calculations of diffuse scattering patterns is given in the Bloch-wave scheme. The time average on the thermal vibration configurations and statistical structure average over imperfections have been performed analytically before numerical calculation.

A rigorous theoretical proof is given to show that the inclusion of the complex potential in the dynamical calculation automatically recovers the contributions made by the high-order diffuse scattering, although the calculation is done using the equation derived for single diffuse scattering. This conclusion gives the basis for extending the conventional diffraction theories developed under the first-order diffuse scattering to cases where the specimen thickness is large and/or the degree of disorder is high.

References

Allen, L. J. & Rossouw, C. J. (1990). *Phys. Rev. B*, **42**, 11644–11654.

Amelinckx, S. & Van Dyck, D. (1993). *Electron Diffraction Techniques*, Vol. 2, edited by J. M. Cowley, pp. 309–371. International Union of Crystallography/Oxford University Press.

Anderson, P. W. & Hasegawa, H. (1955). *Phys. Rev.* **100**, 675–683.

Becker, P. & Al Haddad, M. (1990). *Acta Cryst.* A**46**, 123–129.

Becker, P. & Al Haddad, M. (1992). *Acta Cryst.* A**48**, 121–134.

Bethe, H. A. (1928). *Ann. Phys. (Leipzig)*, **87**, 55–129.

Bird, D. M. & King, Q. A. (1990). *Acta Cryst.* A**46**, 202–209.

Borie, B. (1957). *Acta Cryst.* **10**, 89–96.

Borie, B. (1959). *Acta Cryst.* **12**, 280–282.

Coene, W. & Van Dyck, D. (1990). *Ultramicroscopy*, **33**, 261–267.

Cowley, J. M. (1950). *Phys. Rev.* **77**, 669–675.

Cowley, J. M. (1988). *Acta Cryst.* A**44**, 847–855.

Cowley, J. M. (1992). Editor. *Electron Diffraction Techniques*, Vol. 1. International Union of Crystallography/Oxford University Press.

Cowley, J. M. (1993). Editor. *Electron Diffraction Techniques*, Vol. 2. International Union of Crystallography/Oxford University Press.

Cowley, J. M. (1995). *Diffraction Physics*, 3rd revised edition, chs. 7, 17. Amsterdam: Elsevier.

Cowley, J. M. & Moodie, A. F. (1957). *Acta Cryst.* **10**, 609–619.

Cowley, J. M. & Pogany, A. P. (1968). *Acta Cryst.* **24**, 109–116.

Dai, Z. R., Wang, Z. L., Chen, Y. R., Wu, H. Z. & Liu, W. X. (1996). *Philos. Mag.* **73**, 415–425.

Dai, Z. R., Wang, Z. L. & Liu, W. X. (1996). *Philos. Mag.* In the press.

De Gennes, P. G. (1960). *Phys. Rev.* **118**, 141–154.

De Meulenaere, P., Van Dyck, D., Van Tendeloo, G. & Van Landuyt, J. (1995). *Ultramicroscopy*, **60**, 171–185.

De Ridder, R., Van Tendeloo, G. & Amelinckx, S. (1976). *Acta Cryst.* A**32**, 216–224.

Dinges, C., Berger, A. & Rose, H. (1995). *Ultramicroscopy*, **60**, 49–70.

Doyle, P. A. & Turner, P. S. (1968). *Acta Cryst.* A**24**, 390–397.
Dudarev, S. L., Peng, L. M. & Ryazanov, M. I. (1991). *Acta Cryst.* A**47**, 170–176.
Dudarev, S. L., Peng, L. M. & Whelan, M. J. (1992). *Surf. Sci.* **279**, 380–394.
Dudarev, S. L., Peng, L. M. & Whelan, M. J. (1993). *Phys. Rev. B*, **48**, 13408–13429.
Dudarev, S. L., Vvedensky, D. D. & Whelan, M. J. (1993). *Phys. Rev. B*, **50**, 14525–14538.
Fanidis, C., Van Dyck, D., Coene, W. & Van Landuyt, J. (1989). *Computer Simulation of Electron Microscope Diffraction and Images*, edited by W. Krakow & M. O'Keefe, pp. 135–157. Warrendale, PA: The Minerals, Metals and Materials Society.
Fanidis, C., Van Dyck, D. & Van Landuyt, J. (1992). *Ultramicroscopy*, **41**, 55–64.
Flinn, P. A. (1956). *Phys. Rev.* **104**, 350–356.
Gjønnes, J. (1993). *Electron Diffraction Techniques*, Vol. 2, edited by J. M. Cowley, pp. 223–259. International Union of Crystallography/Oxford University Press.
Hall, C. R. (1965). *Philos. Mag.* **12**, 815–826.
Hall, C. R. & Hirsch, P. B. (1965). *Proc. R. Soc. London Ser. A*, **286**, 158–177.
Hayakawa, M. & Cohen, J. B. (1975). *Acta Cryst.* A**31**, 635–645.
Høier, T. (1973). *Acta Cryst.* A**29**, 663–672.
Honjo, G., Kodera, S. & Kitamura, K. (1964). *J. Phys. Soc. Jpn*, **19**, 351–367.
Humphreys, C. J. (1979). *Rep. Prog. Phys.* **42**, 1825–1887.
Jin, S., Tiefel, T. H., McCormack, M., Fastnacht, R. A., Ramech, R. & Chen, L. H. (1994). *Science*, **264**, 413–415.
Jonker, G. H. & van Santen, J. H. (1953). *Physica (Utrecht)*, **19**, 120–130.
Kainuma, Y., Kashiwase, Y. & Kogiso, M. (1976). *J. Phys. Soc. Jpn*, **40**, 1707–1712.
Kato, N. (1980). *Acta Cryst.* A**36**, 763–769, 770–778.
Kato, N. (1991). *Acta Cryst.* A**47**, 1–11.
Komatsu, K. & Teramoto, K. (1966). *J. Phys. Soc. Jpn*, **21**, 1152–1159.
Reimer, L. (1995). Editor. *Energy-Filtering Transmission Electron Microscopy. Springer Series in Optical Sciences*, Vol. 71. New York: Springer.
Rossouw, C. J. (1985). *Ultramicroscopy*, **16**, 241–254.
Rossouw, C. J. & Bursill, L. A. (1985). *Acta Cryst.* A**41**, 320–327.
Spence, J. C. H. (1988). *Experimental High-Resolution Electron Microscopy*, 2d ed, p. 128. Oxford University Press.
Spence, J. C. H. & Zuo, J. M. (1992). *Electron Microdiffraction*. New York/London: Plenum Press.
Takagi, S. (1958). *J. Phys. Soc. Jpn*, **13**, 278–286.
Takagi, S. (1962). *Acta Cryst.* **15**, 1311–1312.
Taupin, D. (1964). *Bull. Soc. Fr. Minéral. Cristallogr.* **87**, 469–511.
Van Dyck, D. (1985). *Adv. Electron. Electron Phys.* **65**, 295–355.
Wang, Z. L. (1990). *Phys. Rev. B*, **41**, 12818–12837.
Wang, Z. L. (1992). *Philos. Mag.* B**65**, 559–587.
Wang, Z. L. (1995*a*). *Elastic and Inelastic Scattering in Electron Diffraction and Imaging*, chs. 6, 7, 10. New York/London: Plenum Press.
Wang, Z. L. (1995*b*). *Acta Cryst.* A**51**, 569–585.
Wang, Z. L. (1996*a*). *Surf. Sci.* In the press.
Wang, Z. L. (1996*b*). *Philos. Mag.* B. In the press.
Wang, Z. L. (1997). *Scan. Microsc.* Submitted.
Wang, Z. L. & Bentley, J. (1991). *Ultramicroscopy*, **38**, 181–213.
Wang, Z. L. & Li, D. C. (1995). *Philos. Mag.* B**71**, 201–219.
Warren, B. E. (1990). *X-ray Diffraction*, ch. 11. New York: Dover.
Weickenmeier, A. & Kohl, H. (1991). *Acta Cryst.* A**47**, 590–597.
Yoshioka, H. (1957). *J. Phys. Soc. Jpn*, **12**, 618–628.
Yoshioka, H. & Kainuma, Y. (1962). *J. Phys. Soc. Jpn*, **17**, Suppl. BII, 134–136.
Zener, C. (1951). *Phys. Rev.* **82**, 403–405.
Zuo, J. M., Spence, J. C. H. & O'Keefe, M. (1988). *Phys. Rev. Lett.* **61**, 353–356.